C. Vázquez and D. S. Montero. "Temperature impairment characterization in radio-over-multimode fiber systems. *Opt. Eng.* 51 (8), 085007 (Aug 08, 2012). ; http://dx.doi.org/10.1117/1.OE.51.8.085007

Temperature impairment characterization in radio-over-multimode fiber systems

David S. Montero
Carmen Vázquez
Universidad Carlos III de Madrid Electronics Technology Department
Avenida de la Universidad 30 28911, Leganés, Madrid, Spain
E-mail: dsmontero@ing.uc3m.es

Abstract. Arbitrary operating conditions, such as the temperature depen-dence in the fiber link impose a challenge for the extension of radio-over-multimode fiber techniques. Temperature impairment characterization is analyzed over the broadband transmission bands that can be present in the frequency response of multimode fiber (MMF) supporting multiple-GHz carriers delivering schemes. Experimental results show that these transmission bands are dramatically influenced by the hysteresis of heating and cooling temperature cycles, respectively. The influence of the MMF graded index exponent tolerance on frequency response at higher bands is also analyzed. And this variation can be directly attributed to environmental temperature changes that could affect the MMF link. Additionally, selective mode-launching schemes combined with the use of narrow line-width optical sources are experimentally demonstrated to enable broadband transmission, not only at short but also at middle-reach distances over MMFs.

Subject terms: multimode fiber; temperature dependence; radio-over-fiber; frequency response.

1 Introduction

Actual trends of increasing speed and coverage in the next-generation access (NGA) services marketplace indicate further deployment of higher-capacity communications technologies well into the foreseeable future, even inside the customer's premises, with the need for short and middle-reach links supporting data rates of 1 and 10 Gbps. It is also a matter of fact that recent interests are focused on high-quality display technologies, such as high-definition (HD), three-dimensional (3-D) visual information, or remote "face-to-face communication", which forecast requirements for data transmission speed more than 40 Gbps by 2020 that can be achievable only with optical networks.[1]

Optical communication systems based on optical fibers allow transmission over long distances at extremely high data rates. Silica-based multimode fiber (MMF) provides the necessary bandwidth for already installed short and middle-reach links at a much lower installation and component cost, compared with their singlemode (SMF) counterpart. As the optical network gets closer to the end user, most of the interconnections are needed and less cost-sharing between users is obtainable making the use of SMF quite impractical. The underlying factor is the fact that the MMF is easier to fabricate, to connect, and to manipulate (allow less stringent alignment tolerances) thanks to its larger core diameter.

On the other hand, wireless technologies are developing fast but there is a need to link base stations/servers to the antenna using fixed links together with the future exploitation of capacities well beyond present day standards, such as IEEE802.11a/b/g or IEEE802.16. This wireless service uses signals at the radio-frequency (RF) level that are analogue in nature, at least in the sense that they cannot be carried directly by digital baseband modulation. At the same time, an emerging theme in NGA research includes seamless wireline-wireless convergence addressed by radio-over-fiber (RoF) technology,[2] and optical cabling solutions offer the possibility for semi-transparent transport through the access network microwave to mm-wave radio carriers commonly employed for creating high-capacity picocell wireless networks. These picocells are a natural way to increase capacity (i.e., to accommodate more users) and to enable better frequency spectrum utilization. Advanced RoF techniques[3] can efficiently generate and transport high frequency carriers, and deliver them to simplified antenna stations. Thus, they can convey high data rates in comprehensive modulation formats on multiple-GHz carriers in MMF networks.

In addition to the inherent bandwidth limitation of MMFs, the frequency response of MMF links depends, in general, on launching conditions, source type, variable link lengths, installation bends, connector offsets, environmental temperature changes, or the introduction of any other component along the link. This fact makes the MMF frequency response unpredictable under arbitrary operating conditions and imposes a great challenge for the extension of this bandwidth-dependent radio-over-multimode fiber (RoMMF) performance. Consequently, the potential MMF capacity for communication needs a greater exploitation to meet user requirements for higher data rates and to support the emerging multimedia applications, even more with the inclusion of wireless signals over MMF. To enable the design and utilization of MMFs with such enhanced speeds and signal characteristics, the development of an accurate frequency model is of prime importance. From most of the published models, a method relying on the propagation electric field signals has emerged[4,5] which takes into account most of

the aforementioned factors that affect the MMF frequency response.

In this paper, the impact of temperature in the frequency response of a RoMMF link is theoretically evaluated and experimentally tested. In Sec. 2, a brief description of the theoretical model is presented. Moreover, the conditions and capability of developing MMF broadband transmission are revisited by means of different sets of theoretical simulations as well as experimental measurements. Section 3 contains temperature impairment characterization analysis over the broadband transmission bands that are present, under certain operating link conditions, in the frequency response performance of MMF, thus contributing to fault link prevention. Finally, the main conclusions of this work are reported in Sec. 4.

2 Broadband Transmission in Silica-Based Multimode Optical Fibers

Novel techniques to expand the MMF capabilities are continuously reported demonstrating that the frequency response of MMF does not diminish monotonically to zero after the baseband bandwidth, but tends to have repeated passbands beyond that.[6] These high-order passbands (or secondary lobes in the frequency spectrum) and flat regions have been used to transmit independent streams of data (digital or analogue) complementary to the baseband bandwidth to exceed the aggregated transmission capacity of MMF,[7] as well as to transport microwave and millimeter-wave radio carriers, commonly employed for creating high-capacity picocell wireless networks in RoF systems, as in Ref. 8.

2.1 *Silica-Based MMF Transfer Function Simulations*

Frequency response simulations versus different parameters are developed to determine optimal conditions for higher transmission bandwidths in baseband, and to investigate the potentials for broadband transmission in regions far from baseband. The MMF frequency response theoretical model is based on the electric field propagation method and has been widely reported in literature.[4,5,9] Simulations are focused on frequency response versus fiber graded index exponent (α) tolerances, and core and cladding refractive indices changes. These factors are critical in the stability of the MMF frequency response performance, and their variation can be directly attributed to environmental temperature changes that could affect the MMF link. Other factors, such as the link length or source linewidth, delimit broadband band range.

A $62.5/125\ \mu$m graded-index multimode fiber with SiO_2 core doped with 6.3mol-% of germanium (GeO_2) and intrinsic attenuation of 0.55 dB/km@1300 nm and 0.35 dB/km@1550 nm, respectively, has been considered for the simulations. Graded refractive index profile has been approximated by the well-known power law equation. Core center and cladding refractive indices are found to be $n_1 = n_1(0,\lambda) = 1.4558$ and $n_2 = 1.4472$, respectively, at a 1300-nm wavelength, from the Sellmeier coefficients provided by the manufacturer. The mode coupling coefficient G_{mm} has been defined by a Gaussian autocorrelation function with a root mean square deviation of $\sigma = 0.0005$, and a correlation length of $\varsigma = 150 \cdot a$, with a being the core radius. It has been assumed a free chirp source and an overfilled launch (OFL) condition (i.e., uniform excitation) with light injection coefficient $C_{\text{mm}} = 1/\text{M}$, with M being the total number of mode groups. Differential mode attenuation (DMA) effects have been simulated using the empirical function reported in Ref. 10, setting parameters $\rho = 9$ and $\eta = 7.35$.

An important aspect is the great dependence of the broadband RoF transmission in the microwave and mm-wave regions on graded index exponent profile tolerances. One percent graded index exponent deviations have been simulated, and the results are shown on Fig. 1 for a 2-km-long fiber link. Significant displacements on the high-order resonances over the frequency spectrum are observed. From simulation conditions illustrated in Fig. 1(b) an increase of $\alpha' = \alpha + 0.04$ produces a change on the first order resonance of 3.2 GHz if we compare cases $\alpha = 2.02$ and $\alpha = 2.06$. This fact could cause a serious MMF link fault if multiple-GHz carriers are intended to be transmitted through this physical medium when performing a RoMMF system. A 1300-nm Fabry-Perot (FP) laser with 5.5 nm linewidth has been considered. It should be mentioned that graded index exponent tolerances considered

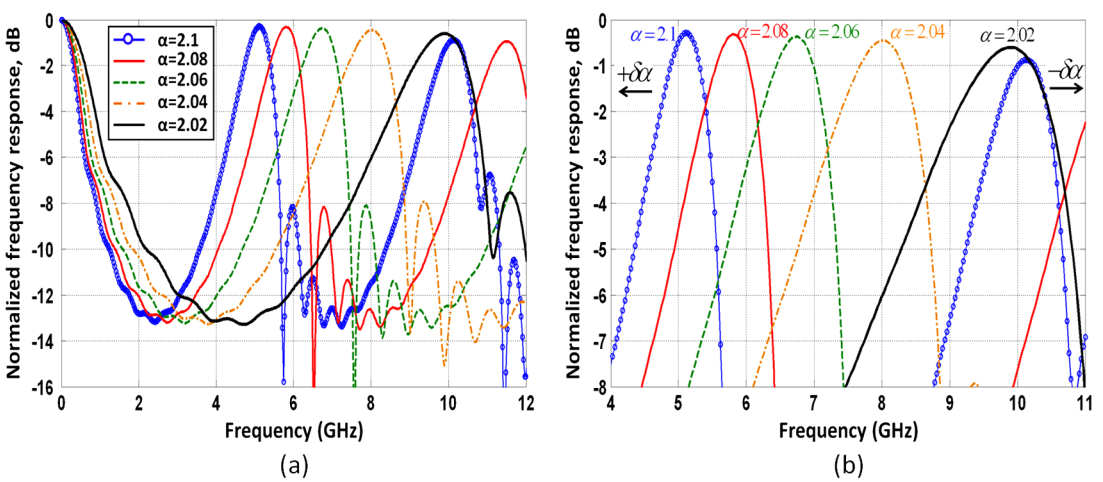

Fig. 1 (a) Frequency response of a 2-km-long MMF fiber link when considering different graded index exponents, α. (b) Zoom of Fig. 2(a) for a frequency span from 4 to 11 GHz.

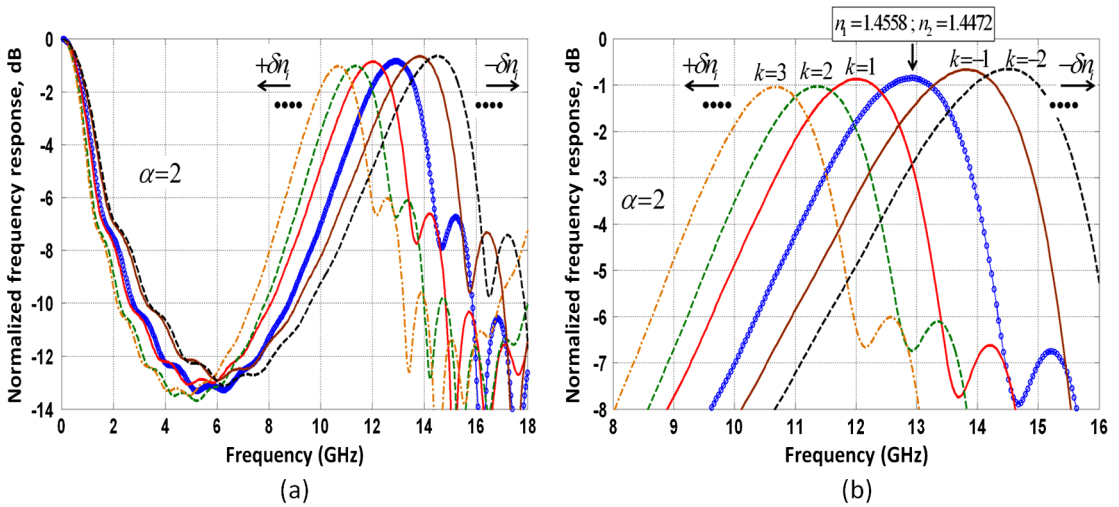

Fig. 2 (a) Influence of core and cladding refractive indices tolerance on the frequency response of a 2-km-long MMF fiber link. (b) Zoom of Fig. 3(a) for a frequency span from 8 GHz to 16 GHz.

on Fig. 1 are lower than those measured and reported by other authors,[11] so impairment effect can be even higher. For instance, in Fig. 7 of Ref. 11, a total α deviation of $|0.09|$ was experimentally measured by interferometric techniques in a range of temperature between 21°C and 61°C. This fact corresponds to a 4.6% graded index exponent deviation for the temperature range considered with a thermal coefficient, assuming a linear approach, of 2×10^{-3}°C^{-1}. Although authors in their work consider this deviation as negligible for their application, it is theoretically demonstrated that this fact could seriously affect the broadband RoMMF transmission.

On the other hand, in Fig. 2 the influence of refractive index deviations that could be caused due to temperature variations is analyzed. From this Fig. 2 it is clearly seen that the high-order resonances of the MMF frequency response are also frequency-shifted. It has been assumed a graded-index silica-based MMF in which the core and cladding refractive indices vary following:

$$n_i'(\lambda) = n_i(\lambda) + k \cdot \delta n_i \quad \text{with} \quad k \in \mathrm{Z}. \tag{1}$$

Core center and cladding refractive index tolerances have been assumed to be $\delta n_1 = 2 \times 10^{-3}$ and $\delta n_2 = 1.5 \times 10^{-3}$, respectively. These deviation values are derived from Refs. 11–13 where a core and cladding thermo-optical coefficient,dn_i/dT, of a graded-index silica-based optical fiber was found to be around 10^{-4}°C^{-1} in both cases. In our simulations, the higher tolerance considered for the core refractive index compared with that of the cladding is related to the fact that dopants are usually introduced in the silica fiber core by different deposition techniques. In addition, typical values of $n_1 = 1.4558$ and $n_2 = 1.4472$ have been considered for an optical fiber with silica core doped with a 6.3 mol-% of germanium (GeO_2) at an operating wavelength of 1300 nm. Its corresponding curve, when no refractive index deviation is considered, is also illustrated in Fig. 2 by the solid-circled (-o-) blue line. From this figure, a dramatic variation of the first-resonance central frequency around 20% is observed for a 0.4% core refractive index deviation from the nominal value.

2.2 *Experimental Results*

In this section, some measurement examples of the silica-based MMF transfer function are presented highlighting the conditions upon broadband MMF transmission in regions far from baseband can be featured.

The setup schematic for the experimental measurements is shown in Fig. 3. A lightwave component analyzer (LCA; Agilent 8703B, 50 MHz–20 GHz) has been used to measure the frequency response, using a 100-Hz internal filter. In all cases the laser was externally intensity modulated (IM) with an RF sinusoidal signal up to 20 GHz of modulation bandwidth, by means of an electro-optic (E/O) Mach-Zehnder modulator (model JDSU AM-130@1300 nm and JDSU AM-155@1550 nm). The optical output of the E/O modulator was passed through a 62.5/125-μm silica-based MMF fiber patch cord plus a mode scrambler before being launched to the MMF link. This optical launching scheme provides an OFL condition for light injection. At the receiver, the frequency response is detected using a high-speed PIN photodiode, model DSC30S, from Discovery Semiconductors. It should be mentioned that the experimental results of the silica-based MMF link shown in this section have been calibrated with regards to both the E/O intensity modulator and the photodetector electrical responses, being therefore solely attributed to the MMF fiber. It should be also noted that the ripples observed are caused by reflections in the optical system and are not features of the fiber response, although ferrule connector/angled physical contact (FC/APC) connectors are used to minimize this effect.

Core/cladding 62.5/125-μm-diameter silica-based MMF links of lengths around 6 km (6100 m) and 9 km (9150 m) have been evaluated, showing their normalized frequency response up to 20 GHz in Fig. 4. Three different optical sources have been applied for the experiments. Focusing on Fig. 4(a), as it is expected from the theory, the response for the distributed feedback (DFB) laser (in this case operating at 1550 nm and with a full width half maximum (FWHM; of 100 kHz) behaves relatively flat at high frequencies, with maximum variations of approximately $\pm$1.5 dB with regards to a mean level of 3 dB below the low frequency regime. The frequency response employing a FP laser at 1300 nm with FWHM of 1.8 nm, however,

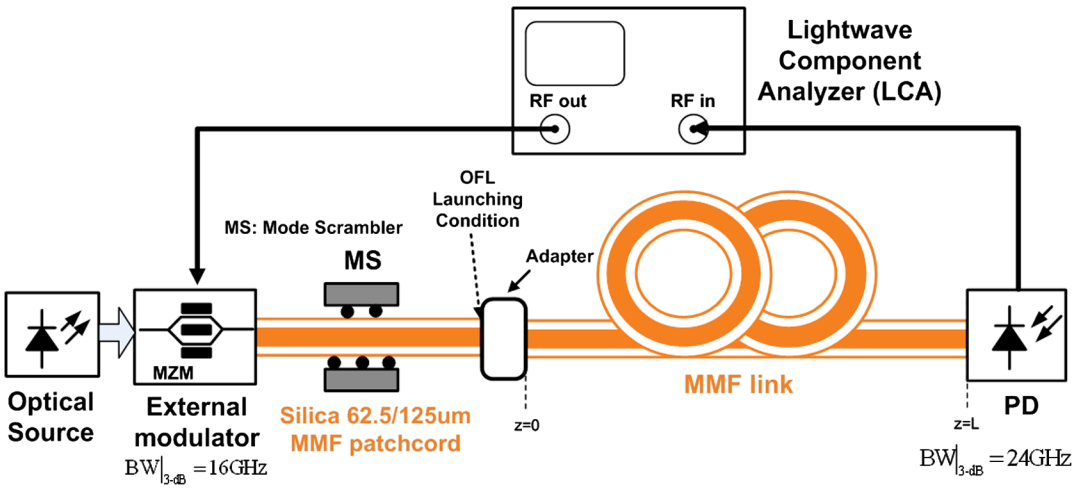

Fig. 3 Block diagram of the experimental setup for the MMF link frequency response measurement, up to 20 GHz.

suffers from a low pass effect, for instance by a 18-dB fall at 20 GHz focusing on the 6-km-long link, and no high-order resonances are observed. In the case of the broadband light source (BLS) with 400-nm spectral range the response falls dramatically after a few GHz. Ripples observed at frequencies above 14 GHz at Fig. 4(b) are due to the low signal level detected, close to the noise floor of the measuring equipment.

By evaluating the results from Fig. 4(a) and 4(b), resonances are clearly seen for the case of the DFB optical source, whereas a higher attenuation is achieved for both the FP and the BLS. Comparing these figures, it is observed that exploiting the possibility of transmitting broadband signals at high frequencies is contingent on the use of narrow linewidth sources. For instance, the presence of high-order resonances and a flat region over 18 GHz in the frequency response of the 9-km-long MMF link for the DFB case, shown in Fig. 4(b), is clearly observed.

Finally, Fig. 5 shows a comparison between the theoretical frequency response and the experimental results showing a relative good agreement. Key issues are the presence of a relatively flat region with mean level of 1.5 dB below the low frequency regime in Fig. 5(a), as well as the presence of high-order resonances suitable for multiple-GHz carrier transmission for the case of Fig. 5(b). Although no accurate agreement can be expected due to the many approximations made in the theoretical analysis, as well as the amount of parameters involved in the frequency response in combination with the uncertainty of some key parameters; the results reveal a relative good agreement in the behavior of the silica-based MMF frequency response compared with the curves predicted by the model. This fact is also noticeable if we attend to the central frequencies of the high-order resonances.

It is worth mentioning that previous frequency response measurements reported cover up to 20 GHz at 1-km link length with 1 dB loss,[14] up to 50 GHz at 500-m link length with 15 dB loss,[15] or up to 20 GHz at 5-km length with 5 dB loss.[16] So these are the first measurements on Si-MMF of product bandwidth lengths up to 180 GHz/Km with 5-dB loss, and showing MMF propagation capability beyond 3-dB bandwidth at longer link lengths.

3 Temperature Impairment Characterization

An important aspect highlighted by the model is the great dependence of the broadband RoF transmission in regions

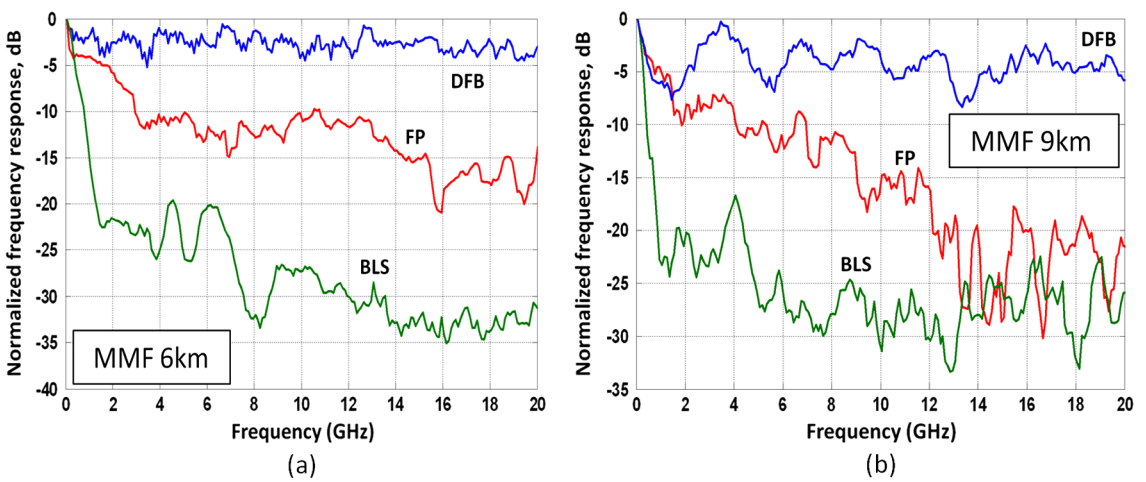

Fig. 4 Measured influence of the optical source linewidth on the frequency response of (a) 6-km-long link; (b) 9-km-long link. DFB laser at 1550 nm, FP laser at 1300 nm.

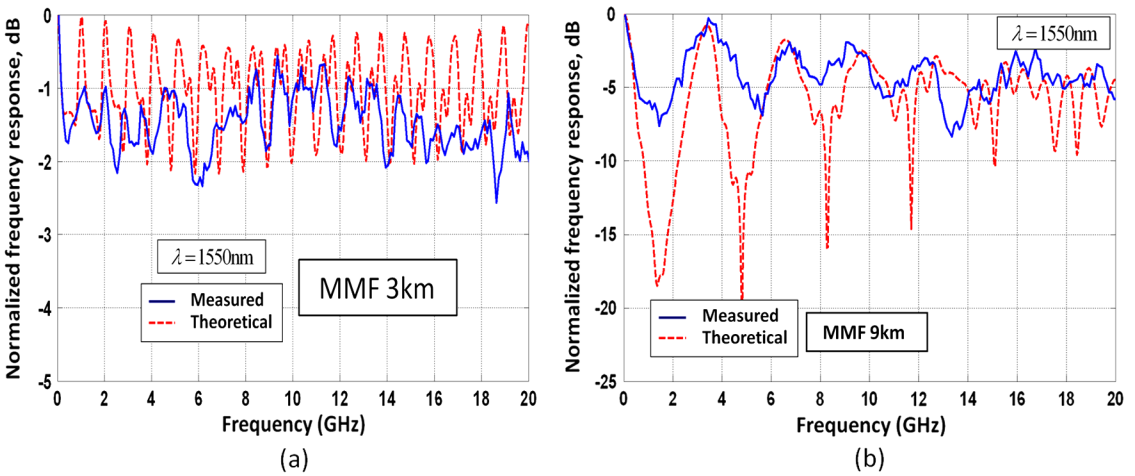

Fig. 5 Theoretical and measured frequency response of 3-km-long (a) and 9-km-long (b) silica-based MMF link with DFB laser source at 1550 nm.

far from baseband on the optical fiber properties. Variations in temperature have also been demonstrated to change some of the optical properties of silica-based MMF, such as the graded index exponent and the refractive indices of both the fiber core and cladding.[11,17,18] For instance, focusing on silica-based optical fibers, a positive thermal coefficient, dn_i/dT of both refractive indices has been observed.[19,20] This fact also imposes a great challenge for the extension of this bandwidth dependent MMF performance and, conse-quently, it is necessary to estimate its effect over the broad-band transmission bands. Up to now, most temperature analysis are devoted to capability of uncooled laser diode to keep linearity in a wide temperature range[21,22] allowing competitive prices of the whole system.

3-dB bandwidth temperature dependence in a 3-km-long silica-based MMF link, when the environmental temperature changes, is experimentally investigated. Going beyond previous works[23] special attention is given to temperature influence on the high-order resonances. Concerning the temperature range selection, having in mind environmental variations, in desert areas thermal amplitude between day and night can go up to 35 ℃, whereas in continental climates like in Madridit oscillates up to 12℃. However, annual thermal amplitude is significant; with a record of 87℃ in extreme continental climate in Mongolia, and in Spain in some regions can easily go beyond 20℃. If in-building applications are considered, building regulations and power efficiency policies can imply thermal amplitudes of 18℃ between occupied and unoccupied periods. And finally, most hub equipment for wireless applications must fulfill operation temperature ranges from 0℃ up to 70℃. And those temperature ranges should also be applied for MMF under consideration. Having all previous constraints in mind, two sets of measurements have been taken with a maximum excursion from $T = 22$℃ (environment) to $T = 80$℃. The hysteresis cycle of the measurements has also been evaluated.

In the first set of measurements, an FP optical source at 1317 nm (model SOF-131-C from Accelink) with 2.7 nm of linewidth, and modulated up to 20 GHz by an external E/O modulator has been used to launch optical power into the fiber via a 2-m-long silica-based MMF patch cord with a mode scrambler thus providing OFL launching condition. The setup follows the same principle as that depicted in Fig. 3. Test equipment was isolated from the heating source, so that only temperature changes relating to the MMF fiber spool were measured. An average factor of 16 for each temperature test measurement was applied. Speckle contrast is considered negligible as in previous works.[24]

Results depicted in Fig. 6 show the normalized frequency response for different temperature cases, only attending to the power offset, i.e., dB fall in the frequency response, when temperature is changing. Figure 6(a) illustrates the normalized measured frequency response for a 3-km-long MMF link (Fujikura FutureGuide® 62.5-μm-core diameter) at $T =$ 28℃ and $T = 78$℃ (maximum temperature tested in this experiment), respectively. The frequency response, in this case, shows slight variations over the spectrum but with power offsets at specific points up to 2 dB, see Fig. 6(a) inset. On the other hand, Fig. 6(b) shows the hysteresis cycle of the same MMF link at $T = 28$℃ (environmental) when heating (forwards) up to 78℃ and then cooling (backwards). From Fig. 6(b) inset, the maximum hysteresis deviation is found to be 3 dB at 3 GHz, compromising the 3-dB baseband bandwidth. In both cases, an average has been applied, with averaging factor Avg = 16.

Considering the above discussion it is also expected that temperature seriously affect the location of the high-order resonances for the implementation of a RoMMF system. Consequently, the variation on the performance of the frequency response of an arbitrary single secondary side-lobe with regards to this impairment is evaluated. For this latter case, similar tests of frequency response temperature dependence and hysteresis as above were performed at OFL condition but employing a DFB laser source operating at 1550 nm with 100 kHz of source linewidth. With such a link configuration high-order resonances can be clearly appreciated, see Fig. 4(b). Temperature variations ranged from $T = 22$℃ (environment) to $T = 80$℃. The following set of pictures comprising Fig. 7 is referred to the first-order resonance, which appears in the frequency response of a 9-km-long silica-based MMF link. This resonance is centered around $f_o|_1 = 3.5$ GHz with a 3-dB bandwidth of 2.5 GHz, approximately. This selection allows spectrum allocation in the RoF link of two wireless LAN access points (AP) configured for IEEE 802.11b operation in the 2.4-GHz

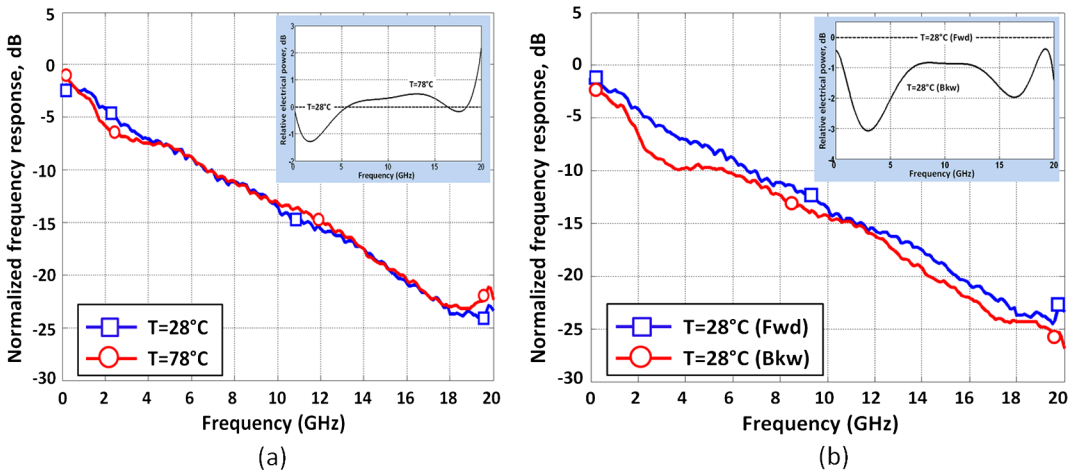

Fig. 6 (a) Experimental frequency response of a 3-km-long silica-based MMF link, at $T = 28°C$ and $T = 78°C$, Avg: averaging factor Avg = 16. (b) Hysteresis of the MMF link at environmental temperature, Avg = 16. Fwd:forward; Bkw:backward. Inset: averaged optical power received, normalized to environmental temperature, $T = 28°C$, Avg = 16.

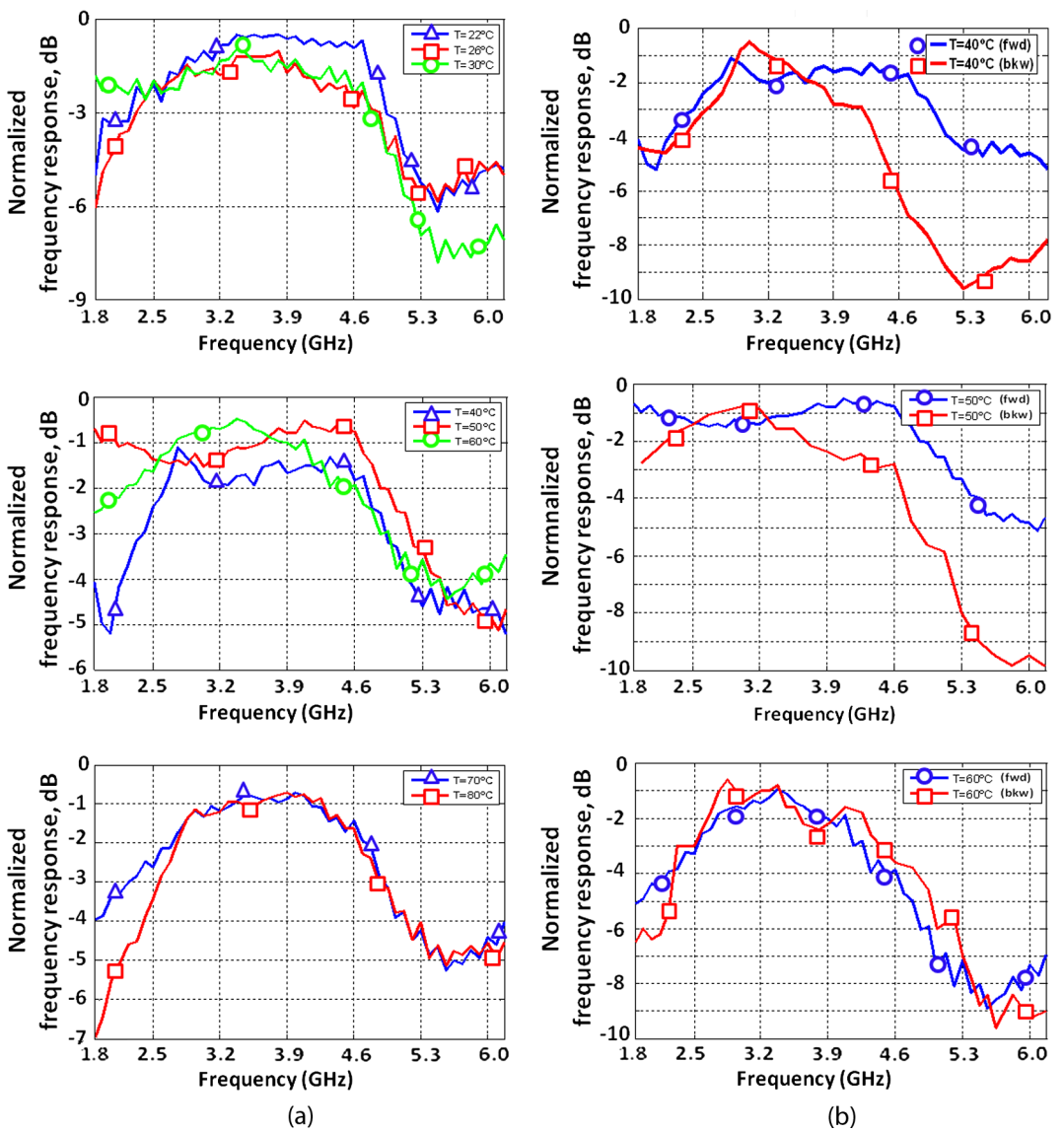

Fig. 7 (a) Measured 9-km-long MMF link first-resonance frequency response from $T = 22°C$ to $T = 80°C$. (b) Hysteresis of the first-resonance at environmental temperature. Fwd: forward; Bkw: backward.

Table 1 First-order resonance temperature dependence performance (fwd) of the MMF link considered.

	First-resonance thermal performance						
Temperature (°C)	22°C	30°C	40°C	50°C	60°C	70°C	80°C
$f_o\|_1$ (GHz)	3.7	3.6	3.6	3.5	3.4	3.6	3.7
$\Delta f_o\|_1\|_{-3\,\mathrm{dB}}$ (GHz)	2.4	2.6	2.6	2.7	2.5	2.3	2.1

band and the other for IEEE 802.lla operation in the 5.2-GHz band.

Figure 7 depicts the performance of the first-resonance that appears in the frequency response of a 9-km-long MMF link. Both figures show the optical power deviations detected for a single sweep measurement. From Fig. 7(a) it can be observed that the central frequency of the first-order resonance show almost no dependence with temperature whereas its 3-dB bandwidth suffers from slight deviations depending on temperature. Results show a nominal 3-dB first-resonance bandwidth of 2.5 ± 0.3 GHz, which means a deviation of $\pm 12\%$ from the nominal value. Conversely, results concerning hysteresis show that high-dependence on temperature cycles of heating (forward) and cooling (backward) is noticeable. In the hysteresis cycle, variations of the 3-dB first-resonance bandwidth up to ± 0.6 GHz (which means a deviation of 24%) were achieved. Furthermore, first-resonance central frequency was displaced even 0.5 GHz, which means a deviation of 14% from the aforementioned value of 3.5 GHz obtained.

Table 1 summarizes the first-order resonance measured 3-dB bandwidth ($\Delta f_o|_1|_{-3\,\mathrm{dB}}$) and central frequency ($f_o|_1$) at the different tested temperatures in the forward (fwd) cycle. A statistical analysis of reported measurements show that 3-dB bandwidth versus temperature can be approximated by $\{f_{\downarrow}[0, 1(3\ \mathrm{dB})][T] = 1,73012 + 0,0405611T - 0,000453778T\uparrow 2\}$ being T in ℃ for a range between 20℃ up to 80℃, and 3-dB bandwidth in GHz. This approximation has a standard deviation of 0.05887 GHz.

It should be outlined that a thermal coefficient of around 1.5×10^{-4}℃$^{-1}$ for the core and cladding refractive indices, respectively, has been reported by several authors[11,19,20,25] but having a negligible influence on the frequency response (and so on the high-order resonances) for the temperature ranges considered, and simulations with the model reported here are consistent with this fact. In contrast, for a similar temperature range, deviations of around units (in percentage from the nominal value)of the graded index exponent α,due to the influence of temperature on the silica properties, have been reported.[11,13] Consequently, the slight variations on the 3-dB first-resonance bandwidth observed in Table 1 can be mainly attributed to the great dependence of the MMF frequency response on the graded index exponent profile tolerances.

4 Conclusions

Transmission of multiple-GHz carriers in silica-based MMF links can be featured at certain frequencies enabling the extension of broadband transmission, albeit a small power penalty. In this work, this fact has been theoretically and experimentally revisited. However, the potentials of MMF to support broadband RF, microwave, and millimeter-wave transmission over short, intermediate, and long distances are yet to be fully known, as its frequency response seems to be unpredictable under arbitrary operating conditions as well as fiber characteristics. Temperature impact on bands far from baseband for high-speed data rate applications in RoMMF systems has been demonstrated.Central frequencies of the high-order resonances as well as their 3-dB bandwidths have been experimentally verified to show little dependence (less than 10% deviation) with environmental temperature changes. However, it has been tested a high-dependence of the transmission bands on temperature cycles of heating (forward) and cooling (backward). It has been demonstrated that an accurate addressing of these resonances in the frequency response is needed to maximize the performance of RoMMF broadband transmissions.

Acknowledgments

This work was supported by Spanish CICyT project TEC2009-14718-C03-03 from the Spanish Ministry of Science, and by project FACTOTEM-II-CM: S2009/ESP-1781 of ComunidadAutónoma de Madrid.

References

1. T. Toma et al., "Dual full high definition 3D video real-time communication system," in *Proc. Int. Conf. Plastic Opt. Fibers (ICPOF)*, Bilbao, Spain, pp. 475–479 (2011).
2. M. C. Parker et al., "Radio-over-fibre technologies arising from the building the future optical network in Europe (BONE) project," *IET Optoelectron.* **4**(6), 247–259 (2010).
3. A. M. J. Koonen and M. GarciaLarrodé, "Radio-0ver-MMF techniques Part II: microwave to millimeter-wave systems," *J. Lightwave Technol.* **26**(15), 2396–2408 (2008).
4. I. Gasulla and J. Capmany, "Transfer function of multimode fiber links using an electric field propagation model: application to radio over fibre systems," *Opt. Express* **14**(20), 9051–9070 (2006).
5. D. S. Montero and C. Vázquez, "Analysis of the electric field propagation method: theoretical model applied to perfluorinated graded-index polymer optical fiber links," *Opt. Lett.* **36**(20), 4116–4118 (2011).
6. J. D. Ingham et al., "Bidirectional transmission of 32-QAM radio over a single multimode fibre using 850-nm vertical-cavity half-duplex transceivers," in *IEEE Proc. 28th European Conf. Opt. Commun. (ECOC)*, Brussels, Belgium, pp. 1–2 (2002).
7. I. Gasulla and J. Capmany, "Simultaneous baseband and radio over fiber signal transmission over a 5 km MMF link," in *IEEE Proc. Int. Topics Meeting Microwave Photonics*, Gold Coast, Qld, pp. 209–212 (2008).
8. M. García Larrodé, A. M. J. Koonen, and J. J. Vegas Olmos, "Overcoming modal bandwidth limitation in radio-over-multimode fiber links," *IEEE Photon. Technol. Lett.* **18**(22), 2428–2430 (2006).
9. B. E. A. Saleh and R. M. Abdula, "Optical interference and pulse propagation in multimode fibers," *Fiber Integr. Opt.* **5**(2), 161–201 (1985).
10. G. Yabre, "Theoretical investigation on the dispersion of graded-index polymer optical fibers," *J. Lightwave Technol.* **18**(6), 869–877 (2000).

11. A. A. Hamza et al., "Influence of temperature on the optical and structural properties along the diameter of optical fibers," *Opt. Lasers Eng.* **41**(2), 261–275 (2004).
12. N. Barakat, A. A. Hamza, and A. S. Goneid, "Multiple-beam interference fringes applied to GRIN optical waveguides to determine fiber characteristics," *Appl. Opt.* **24**(24), 4383–4386 (1985).
13. A. A. Hamza et al., "Interferometric studies on the influence of temperature on the optical and dispersion parameters of GRIN optical fibre," *Opt. Lasers Eng.* **45**(1), 145–152 (2007).
14. P. Hartmann et al., "1–20 GHz directly modulated radio over MMF link," in *IEEE Proc. Int Topics Meeting Microwave Photonics*, Seoul, Korea, pp. 95–98 (2005).
15. B. A. Khawaja and M. J. Cryan, "Characterisation of multimode fibres for use in millimetrewave radio-over-fibresystems," in *IEEE Proc. Asia-Pacific Microwave Conf.*, Bangkok, Thailand, pp. 1–4 (2007).
16. I. Gasulla and J. Capmany, "Transmission of high-frequency radio over fibre signals through short and middle reach Multimode Fibre links using a low-linewidth laser," in *IEEE Proc. Int. Topics Meeting Microwave Photonics*, Victoria, BC, pp. 116–119 (2007).
17. F. Tarrach, A. Ch'hayder, and S. Guermazi, "Influence of thermal aging on optical fiber properties," *Opt. Eng.* **47**(6), 065006 (2008).
18. A. Ch'hayder et al., "Effect of thermal aging on Rayleigh backscattering in an optical fiber," *Opt. Eng.* **48**(4), 045001 (2009).
19. G. Ghosh, M. Endo, and T. Iwasaki, "Temperature-dependent Sellmeiercoefficients and chromatic dispersions for some optical fiber glasses," *J. Lightwave Technol.* **12**(8), 1338–1342 (1994).
20. C. Z. Tan and J. Arndt, "Temperature dependence of refractive index of glassy SiO2 in the infrared wavelength range," *J. Phys. Chem. Solids* **61**(8), 1315–1320 (2000).
21. J. Ingham et al., "Wide-frequency-range operation of a high-linearity uncooled DFB laser for next-generation radio-over-fiber," in *IEEE Proc. Opt. Fiber Commun. Conf. (OFC)*, Atlanta, Georgia, Vol. **2**, pp. 754–756 (2003).
22. A. J. Seeds and T. Ismail, "Broadband access using wireless over multimode fiber systems," *J. Lightwave Technol.* **28**(16), 2430–2435 (2010).
23. D. S. Montero et al., "Experimental analysis of temperature dependence in multimode optical fiber links for radio-over-fiber applications," in *IEEE Proc. 11th Int. Conf. Transparent Optical Networks (ICTON)*, Ponta Delgada, Portugal, pp. 1–4 (2009).
24. I. Gasulla and J. Capmany, "Modal noise impact in radio over fiber multimode fiber links," *Opt. Express* **16**(1), 121–126 (2008).
25. N. Shibata, S. Shibata, and T. Edahiro, "Refractive index dispersion of lightguide glasses at high temperature," *Electron. Lett.* **17**(8), 310–311 (1981).